Journal of Materials Chemistry B

Supramolecular hydrogels co-loading camptothecine and doxorubicin for sustainedly synergistic tumor therapy

Journal:	*Journal of Materials Chemistry B*
Manuscript ID:	TB-ART-11-2014-001971.R1
Article Type:	Paper
Date Submitted by the Author:	21-Jan-2015
Complete List of Authors:	Zhang, Wei; Jinan University, zhou, Xiaoyan; Jinan University, Department of biomedical engineering Liu, Tao; Southern Medical University, Ma, Dong; Jinan University, Department of Biomedical Engineering Xue, Wei; Jinan University,

Supramolecular hydrogels co-loading camptothecine and doxorubicin for sustainedly synergistic tumor therapy

Wei Zhang [a,1], Xiaoyan Zhou [a,1], Tao Liu [b], Dong Ma [a,*], Wei Xue [a,*]

[a] Key Laboratory of Biomaterials of Guangdong Higher Education Institutes, Department of Biomedical Engineering, Jinan University, Guangzhou 510632, China

[b] Department of Otolaryngology, Zhujiang Hospital, Southern Medical University, Guangzhou 510282, China

[1] The authors contributed equally to this work.

E-mail: tmadong@jnu.edu.cn (Dr. D. Ma); Tel/Fax: + 86 20 85224338

weixue_jnu@aliyun.com.cn (Prof. W. Xue); Tel/Fax: + 86 20 85224338

Abstract

The co-delivery of multidrug has become the primary strategy in cancer therapy in recent years, because this technique could promote the synergistic actions, reduce the side effects and deter the development of drug resistance. To achieve a controlled and sustained release of the loaded drugs, a supramolecular hydrogel based on the host-guest interactions between hyperbranched polyglycerol derivative and α-cyclodextrin was prepared and used to co-load camptothecine and doxorubicin for sustainedly synergistic tumor therapy. The gelation kinetics, hydrogel strength and supramolecular structure of the obtained hydrogel were studied by dynamic and steady rheometry under various concentrations of *α*-CD. The sustained dual drug release from supramolecular hydrogel *in vitro*, and their synergistic effect *in vitro* and *in vivo* were also explored. Moreover, the supramolecular hydrogel showed a receivable blood compatibility and non-cytotoxity by *in vitro* and *in vivo* assays. Therefore, this supramolecular hydrogel suggested a potential application in sustainedly synergistic tumor therapy.

Key words: supramolecular hydrogel, sustained dual drug release, synergistic therapy

1. Introduction

The co-delivery of multidrug has become the primary strategy in cancer therapy in recent years, because this technique could promote the synergistic actions, reduce the side effects and deter the development of drug resistance [1]. Some traditional drug carriers, such as liposome, micelles, polymers, hybrid nanoparticles etc. have been reported as the co-delivery carriers [2-6].

Hydrogels have attracted a wide range of attention in the field of biomedicine and bioengineering because of their hydrophilic character and potential to be biocompatible [7-9]. Besides of the applications in tissue engineering, there has been an increasing interest in the development of hydrogel matrices for the co-delivery of different therapeutic agents, trying to achieve a controlled and sustained release of the loaded drugs. For example, Seo et al. [10] prepared the chitosan-based hydrogels for the co-delivery of granulocyte colony-stimulating factor and an anticancer drug, and found that such an attempt could exert a more profound anti-tumor effect than does the single delivery of a cancer drug. Patil et al. [11] prepared a riboflavin-based hydrogel for vascular endothelial growth factor and siRNA co-delivery, which showed a good uptake and intracellular release for siRNA. Mao et al. [12] conjugated dipeptide or tripeptide with dexamethasone and two complementary anti-cancer drugs. The obtained gelators could form a co-delivery hydrogel system with the drugs encapsulated in situ.

However, most reported hydrogels above need rigorous reactive condition and long formation time, and the used initiator and crosslinking agent may be adverse to the biocompatibility of hydrogels. The supramolecular hydrogels based on the host-guest interactions between α-cyclodextrin (α-CD) and PEGlated polymeric guest molecules have sparked increasing interest in recent years. This kind of hydrogels could be prepared in a mild condition without organic solvents and other chemical reagents, and their physical properties could be easily modulated [13-15]. Up to know, a considerable amount of literature has been reported for their applications in drug delivery [16-18]. As well known, most antitumor drugs are hydrophobic, which are not easily encapsulated into hydrophilic hydrogel matrix with high loading amount. Ma et al. [19] encapsulated camptothecin (CPT) and granulocyte colony-stimulating factor into a supramolecular hydrogel to achieve the result of limiting side effects to granulocytes as chemotherapy is carrying out. They used the amphiphilic Pluronic F-127 to load hydrophobic CPT, and then interact with α-CD to form the hydrogel. However, the CPT-loading amount was as low as 0.268 mg/g. To enhance the

hydrophobic drug loading and the stability of this supramolecular hydrogel, some new structure design for guest molecules must be carried out.

Hyperbranched polymers are highly branched, polydisperse, three-dimensional macromolecules. Compared to other linear analogues, hyperbranched polymers are expected to have different properties, such as a huge number of modifiable surface functionalities, lower viscosities, and better solubility in water [20]. The polyether backbone of hyperbranched polyglycerol (HPG), taking the biocompatibility of polyether structures such as PEG into account [21], makes it an attractive polymer for biomedical and pharmaceutical applications. This spherical molecule bears hydroxyl groups on the periphery, allowing modification for end user purposes like many other hyperbranched polymers.

Herein, a supramolecular hydrogel based on the amphiphilic hyperbranched polyglycerol (HPG) derivative and α-CD was prepared and used to co-load CPT and doxorubicin (DOX), which are two clinical antitumor drugs (Scheme 1). The used HPG derivative could not only increase the CPT loading amount resulting from its hyperbranched structure, but also confirmed the good blood compatibility of obtained hydrogels due to the more excellent blood compatibility of HPG than PEG. In particular, the gelation kinetics and hydrogel strength of the obtained hydrogels have been studied by dynamic and steady rheometry under various concentrations of *α*-CD, which enabled us to understand and modulate the supramolecuar gelation process. Moreover, the hydrogels have also been investigated with respect to their controlled dual drug release characteristics, and their combination application in cancer therapy *in vitro* and *in vivo*.

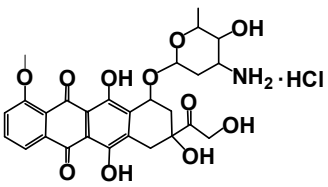

Doxorubicin hydrochloride (DOX)

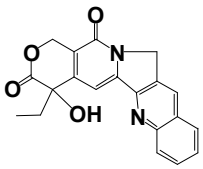

Camptothecin (CPT)

Scheme 1. Chemical structures of DOX and CPT.

2. Experimental section

2.1 Materials

Trimethyloyl propane and glycidol were purchased from Sigma, and glycidol was purified by vacuum distillation before use. Poly(ethylene glycol) methyl ether (MPEG) with the molecular weight of 5000 was purchased from Sigma and used after drying in vacuo at 60°C for 24 h. ε-Caprolactone (ε-CL) was purchased from Sigma and dried by CaH_2 for 24 h. Stannous octoate (Sigma, USA) and α-Cyclodextrin (TCI, Japan) were used as received. Succinic anhydride, camptothecin (CPT), doxorubicin hydrochloride (DOX), dicyclohexylcarbodiimide (DCC) and 4-dimethylaminopyridine (DMAP) were purchased from Aladdin (China) without further purification. All other chemicals used were analytical grade and used as purchased without further purification.

2.2 Synthesis of guest molecules (HPG-PCL-MPEG)

2.2.1 Synthesis of MPEG-PCL-COOH

MPEG-PCL block copolymer was synthesized firstly according to our previous report [22]. Briefly, 2.0 g ε-CL, 5.0 g MPEG and stannous octoate (0.2 wt % of ε-CL) were added into dry flask, and then the mixture was degassed and heated to 110°C. After stirring for 12 h, the content was cooled to room temperature. The product was dissolved in methylene chloride and then precipitated in ethyl ether. The block copolymer was filtered and dried overnight under vacuum with a yield of 92%.

For MPEG-PCL carboxylation, 7.0 g MPEG-PCL, 0.6 g succinic anhydride and 0.72 g DMAP were dissolved in 50 mL dry toluene, and then heated to 40°C for 24 h under argon atmosphere. After that, the solution was precipitated in ethyl ether and dried overnight under vacuum, then MPEG-PCL-COOH was obtained with a yield of 82%. ^{1}H NMR ($CDCl_3$): δ (ppm) 3.65 (s, 454H, CH_2CH_2O), 2.8 (s, 4H, OCCH_2CH_2COOH), 4.08 (m, 30H, $COCH_2CH_2CH_2CH_2CH_2O$), 2.35 (m, 30H, $COCH_2CH_2CH_2CH_2CH_2O$), 1.65 (m, 60H, $COCH_2CH_2CH_2CH_2CH_2O$), 1.40 (m, 30H, $COCH_2CH_2CH_2CH_2CH_2O$).

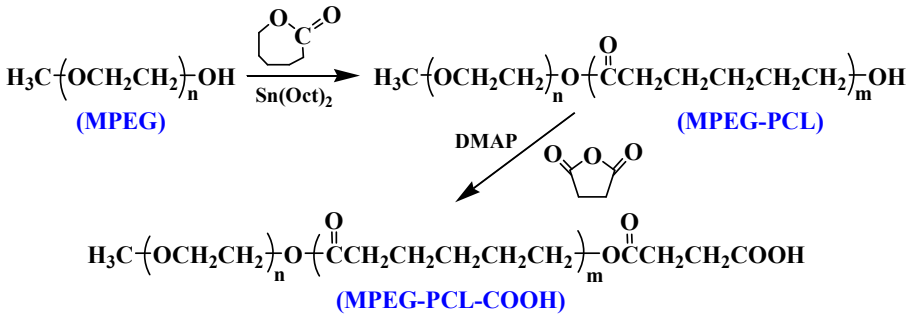

Scheme 2. Synthesis routes to MPEG-PCL-COOH.

2.2.2 Synthesis of HPG

HPG was synthesized according to the reported method [23]. Briefly, trimethyloyl propane (TMP, 120 mg) and 0.1 mL potassium methylate solution in methanol (20 wt%) were added to the flask under argon atmosphere. The mixture was stirred for 15 min after which excess methanol was removed in a vacuum. Then the mixture was heated to 95°C and 5.5 mL glycidol was added dropwise over a period of 12 h using a syringe pump. The product was dissolved in methanol and neutralized through a cationic exchange column (Amberlite IRC-150). Methanol was removed and the obtained HPG was then dialyzed for three days (MWCO = 1000). ^{1}H NMR (D_2O): δ (ppm) 3.5 (m, 390H, CH_2 from HPG), 0.85 (s, 3H, CH_3 from TMP).

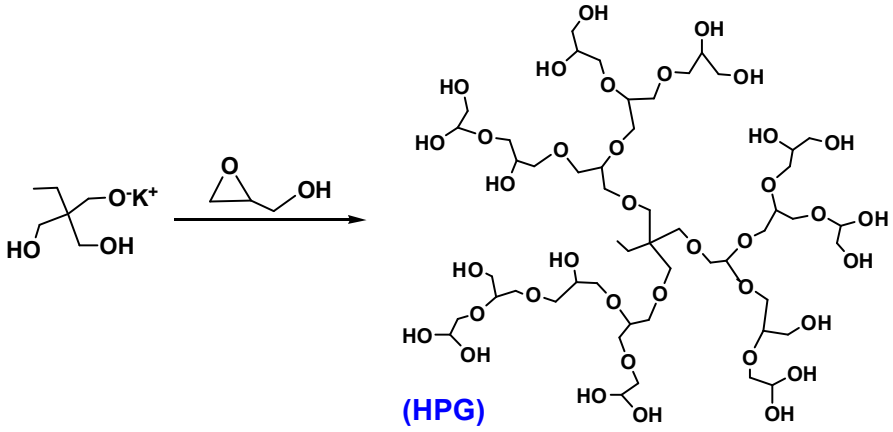

Scheme 3. Synthesis route to HPG.

2.2.3 Synthesis of HPG-PCL-MPEG

For HPG-PCL-MPEG synthesis, 6.0 g MPEG-PCL-COOH and 1.0 g HPG was dissolved in 30 mL dried DMSO, then 0.25 g DCC and 0.13 g DMAP was added. The mixture was stirred at room temperature for 48 h, then dialyzed for three days (MWCO = 8000) and filtrated. The filtrate was frozen to dry to obtain HPG-PCL-MPEG with a yield of 66%.

The chemical structure of HPG-PCL-MPEG was characterized by ^{1}H NMR spectra using DMSO-d6 as the solvent. Gel permeation chromatographic analyses was performed in aqueous solution at 35℃ with an elution rate of 0.6 mL/min on a gel permeation chromatography (GPC) equipped with a Waters 1515 isocratic HPLC pump and a Waters 2414 refractive index detector (Dextran as the standard).

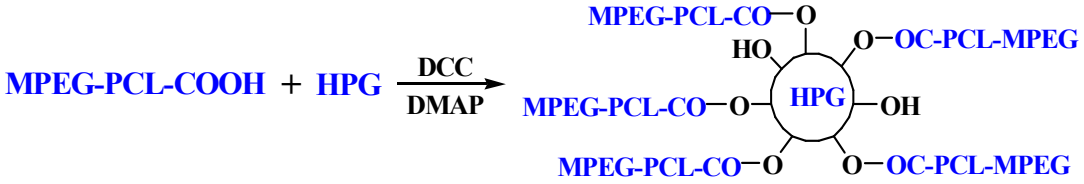

Scheme 4. Synthesis route to HPG-PCL-MPEG.

2.3 CPT-loaded micelles (HPG-PCL-MPEG/CPT)

1.0 g HPG-PCL-MPEG was dissolved in 20 mL distilled water, and then 5 mL CPT acetone solution (0.5 mg/mL) was added dropwise under ice-bath condition. After that, the mixture was stirred at 37°C for 24 h, and the organic solvent was removed by rotary evaporation. The resultant 20 mL mixture was filtered through a 0.45 μm filter to remove free CPT. CPT loading efficiency was studied by UV-Vis spectrophotometer at the absorbance wavelength of 369 nm [24].

2.4 CPT/DOX dual-loaded supramolecular hydrogels

The dual drug-loaded supramolecular hydrogels were prepared by the inclusion complexation of HPG-PCL-MPEG with α-CD in aqueous solution. In a typical experiment, 1 mL HPG-PCL-MPEG/CPT micelle was mixed with 20 μL aqueous DOX solution (1 mg/mL), then equal volume of aqueous α-CD solution (4.0, 6.0 or 8.0 wt.%) was added followed at room

temperature. A gelation occurred to result in a physical network due to the supramolecuar self-assembly between HPG-PCL-MPEG and α-CD.

To investigate the gelation kinetics of aqueous HPG-PCL-MPEG/CPT/DOX/α-CD system, time-sweep rheological analysis was performed by an Advanced Rheometric Extended System (ARES, TA Co.) in oscillatory mode with the parallel plate geometry (20 mm diameter, 1.0 mm gap) at room temperature. In this case, the samples were placed on the plate immediately after the mixing and the measurement began two minutes thereafter. The viscoelastic parameters were measured as a function of time within the linear region previously determined by a strain scan. To investigate the mechanical property of the resultant hydrogels, frequency sweep rheological analysis was conducted with the help of the same ARES. In this case, the hydrogel sample was allowed to consolidate for 12 h before beginning the analysis. The frequency applied to hydrogel sample increased from 0.1 to 100 rad/s with a strain of 0.1%. To confirm the inclusion complex formed from HPG-PCL-MPEG and α-CD, X-ray diffraction measurements were performed by using a Rigaku D/max-2200 type X-ray diffractometer fitted with Ni-filtered Cu Kα radiation with a wavelength of 0.154 nm.

2.5 *In vitro* drug release

To study the in vitro dual-drug release behavior, 200 μL dual-drug-loaded hydrogel samples were immersed in 800 μL phosphate buffer saline (PBS, 0.01 mol/L, pH=7.4) at 37°C and their release profiles were studied. At predetermined time points, 400 μL of the medium solution was taken out and 400 μL fresh PBS was added back to maintain the same total solution volume. The amount of released CPT and DOX were determined according to a method reported previously by a UV pectrophotometer (S52, China) at the absorbance wavelength of 369 and 480 nm [25]. The percentage of cumulative amount of release CPT or DOX was calculated from standard calibration curve. All release studies were carried out in triplicate.

2.6 *In vitro* synergistic effect

To evaluate the synergistic effect of CPT and DOX, MTT assay was performed using HNE-1 cells as previously described with minor modifications [26]. The HNE-1 cells were cultured onto a 96-well plate (5000 cells/well) in complete DMEM (with high glucose and 10% fetal bovine serum

supplemented) culture medium in a humidified atmosphere of 5% CO_2 at 37°C for 24 h. After that, the growth medium was replaced with 100 μL complete DMEM culture medium that contained CPT/DOX micelles with different CPT/DOX concentrations, and five multiple holes were set for every sample. The cell viability of cells treated with individual CPT or DOX was also studied. Cells treated with the same amount of PBS or HPG-PCL-MPEG was used as the control group. The cells were incubated for another 48 h, and the cell viability was assayed by adding 20 μL of MTT (Sigma) PBS solution (5 mg/mL). After incubation at 37°C for another 4 h, the formed crystals were dissolved in 150 μL of dimethyl sulfoxide (DMSO). The absorbance that correlated with the number of viable cells in each well was measured by an MRX-Microplate Reader at a test wavelength of 490 nm.

The synergistic effect of CPT/DOX was evaluated by Chou-Talalay combination index equation [27]:

$$CI = (D)_1/(D_x)_1 + (D)_2/(D_x)_2$$

Where $(D_x)_1$ and $(D_x)_2$ represent the IC_x value of drug 1 alone and drug 2 alone, respectively. $(D)_1$ and $(D)_2$ represent the concentration of drug 1 and drug 2 in the combination system at the CI_x value. Values of CI > 1 represent antagonism, CI = 1 represent additive and CI < 1 represent synergism.

2.7. Cell death assay

HNE-1 cells seeded on the 24-well plates were treated with released CPT, DOX and released CPT/DOX from supramolecular hydrogel composed of 5.0% HPG-PCL-MPEG and 4.0% α-CD (CPT concentration of 0.2 μg/mL and DOX concentration of 0.3 μg/mL) at 37°C for 48 h. Cells treated with PBS and HPG-PCL-MPEG were used as control. At the end of incubation, all cells were trypsinized, collected and resuspended in 200 μL of binding buffer. Thereafter, 5 μL of annexin V-FITC and 10 μL of PI were added and mixed for 15 min in the dark. The stained cells were analyzed using a flow cytometer.

2.8. Synergistic effect *in vivo*

Nude mice implanted with HNE-1 tumors were used as the animal model for *in vivo* anti-tumor test. The mice were divided into 5 groups randomized, each group was 5 mice.

Subsequently, the mice were intratumorally injected with 200 μL PBS (pH=7.4), HPG-PCL-MPEG/α-CD hydrogel, HPG-PCL-MPEG/CPT/α-CD hydrogel, HPG-PCL-MPEG/DOX/α-CD hydrogel and HPG-PCL-MPEG/CPT/DOX/α-CD hydrogel. All groups of mice were injected every 5 days. After 3 weeks, the animals were sacrificed. The Institutional Administration Panel for Laboratory Animal Care approved the experimental design. The university guidelines for care and use of laboratory animals were strictly followed. All animals were housed and fed in the Experimental Animal Center of Jinan University and were specific pathogen free.

2.9 Biocompatibility

2.9.1 Blood compatibility

The blood compatibility of the hydrogel was evaluated by its hemolysis assay. For each sample, its hemolytic potential was tested according to the method reported by O'Leary and Guess [28]. Human blood (0.1 mL) anticoagulated with citrate was added to 5 mL of PBS containing the samples with different concentrations in test tubes. Separate positive (100% hemolysis induced by replacing the PBS with 5 mL of 0.1% Na_2CO_3 solution) and negative (0% hemolysis, PBS with no material added) controls were also set up. Each set of experiments was carried out for three times. All the test tubes containing the samples and the control were incubated for 1 h at 37°C. After the incubation, the tubes were centrifuged at 500 rpm for 5 min. The percentage hemolysis was calculated by measuring the optical density (OD) of the supernatant solution at 545 nm in a UV-Vis spectrophotometer as per the following formula:

Hemolysis(%) = [(OD of the test sample - OD of negative control) × 100]/OD of positive control.

2.9.2 Cell viability

For this test, the hydrogel extracts were first obtained by incubating the supramolecular hydrogel (composed of 5.0% HPG-PCL-MPEG and 4.0% α-CD) in PBS at 37°C over 14 d, and were sterilized together with fresh PBS under Co60 radiation. HNE-1 cells were cultured onto a 96-well plate (5000 cells/well) in complete DMEM (with high glucose and 10% fetal bovine serum supplemented) in a humidified atmosphere of 5% CO_2 at 37°C. After 24 h, the growth medium was replaced with 200 μL complete DMEM culture medium that contained the desired amount of hydrogel extracts. Five multiple holes were set for every sample. The cells treated with the same

amount of PBS were used as a control group. The cells were incubated for another 48 h, and the cell viability was assayed by adding 20 μL of MTT (Sigma) PBS solution (5 mg/mL). After incubation at 37°C for another 4 h, the formed crystals were dissolved in 150 μL of DMSO. The absorbance that correlated with the number of viable cells in each well was measured by an MRX-Microplate Reader at a test wavelength of 490 nm.

2.9.3 *In vivo* toxicity

The HPG-PCL-MPEG/α-CD hydrogel composed of 5.0% HPG-PCL-MPEG and 4.0% α-CD was injected into 5 female BALB/c mice (4-week old, 18 ± 2 g) at the back of the neck (1.0 g/kg mouse), and physiological saline was used as control. After 7 days, all animals were sacrificed, and the liver, heart, spleen, lung and kidney were separated, washed twice with PBS and fixed in 4% formaldehyde for histological examination.

2.10. Statistical analysis

Comparison between groups was analyzed by the one-tailed Student's t-test using statistical software SPSS 11.5. All data are presented as means ± S.D. Differences were considered to be statistically significant when the P values were less than 0.05.

3. Results and discussion

3.1. HPG-PCL-MPEG synthesis and supramolecular hydrogel formation

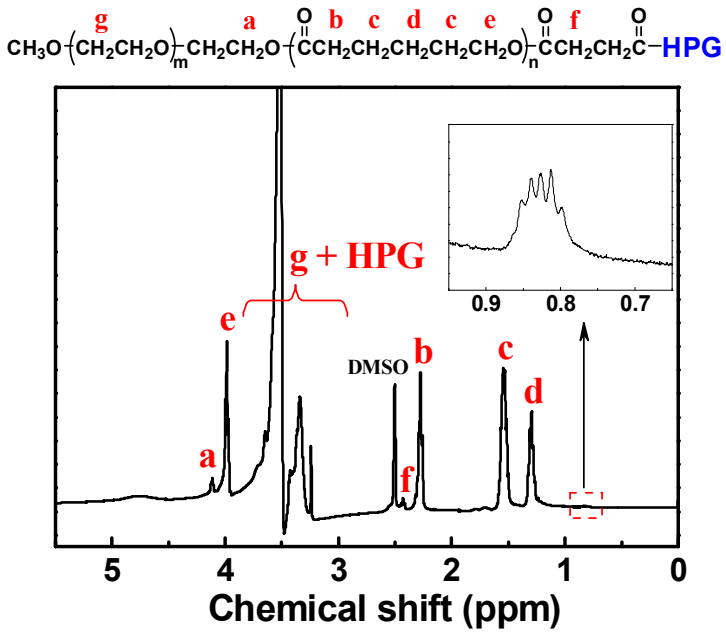

Fig. 1. ^{1}H NMR spectrum of HPG-PCL-MPEG (DMSO-d6, 25°C).

The synthesis routes to HPG-PCL-MPEG were represented in Scheme 2-4, and the obtained HPG-PCL-MPEG was characterized by ^{1}H NMR and GPC. As shown in Fig. 1, the peaks at 1.28, 1.52, 2.25, 2.45, 3.65, 4.02 and 4.15 ppm were attributed to the protons from MPEG-PCL-COOH segments, and the peaks at 0.82 and 3.70 ppm were attributed to the protons from HPG. By calculating the peak area ratio of methylene protons from MPEG (δ = 4.15 ppm) and methyl protons from the core of HPG (δ = 0.82 ppm), it was determined that one HPG molecule was conjugated with an average of 18.6 MPEG-PCL-COOH molecules. The obtained HPG-PCL-MPEG was analyzed by GPC trace and the result was shown in Fig. 2. It was found that HPG-PCL-MPEG and HPG showed the receivable distribution and the elution peak was relatively symmetric, and the molecular weight distribution coefficient (*Mw/Mn*) of HPG-PCL-MPEG was determined to be 1.82.

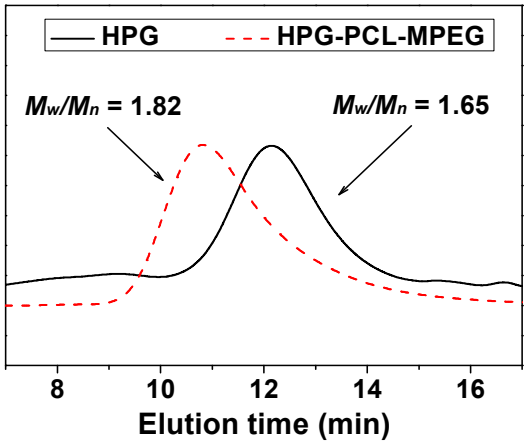

Fig. 2. GPC traces of HPG-PCL-MPEG and HPG (using PEG as the standard sample; 35°C).

For hydrophobic CPT loading, HPG-PCL-MPEG was expected to have a higher loading amount than normal micelles due to its unique hyperbranched topology including the highly branched structures and the spherical shapes [29]. In this work, the loading amount of CPT onto HPG-PCL-MPEG was about 2.8 mg/g determined by HPLC analysis, more than tenfold loading amount than our previous reported carrier [19]. The particle size and morphology of CPT-loaded HPG-PCL-MPEG micelles were shown in Fig. 3. It was found that the micelles have an average size of 128.6 nm, and showed a spherical morphology.

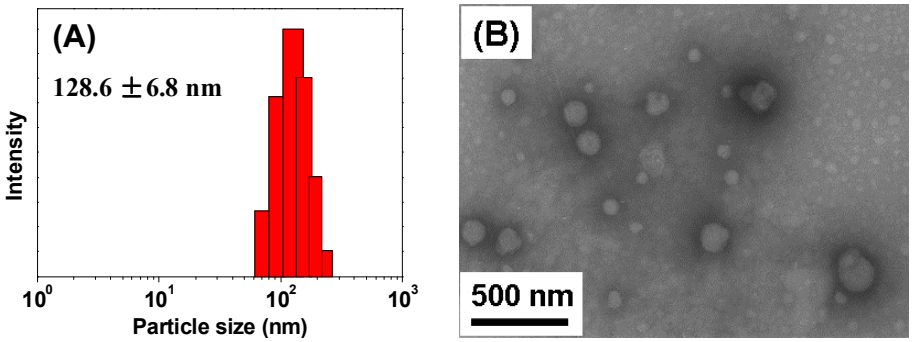

Fig. 3. Particle sizes of CPT-loaded HPG-PCL-MPEG micelles. (B) Typical TEM image of the CPT-loaded HPG-PCL-MPEG micelles.

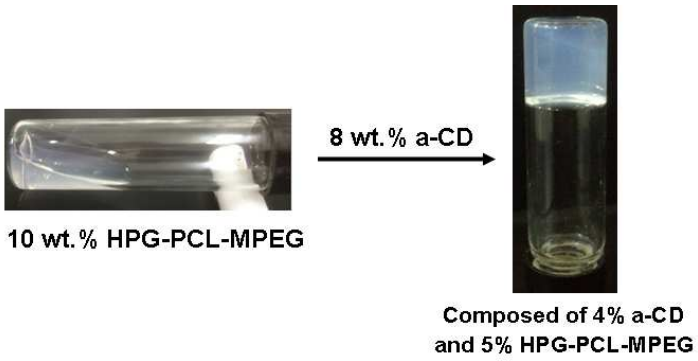

Fig. 4. The photograph for the formation of the supramolecular hydrogel (composed of 5.0% HPG-PCL-MPEG and 4.0% α-CD) at room temperature.

After mixing 10% HPG-PCL-MPEG solution with an equal volume of 8% α-CD solution at room temperature, the mixture could turn to an invertible gel after a determined period (Fig. 4). This phenomenon was attributed to the inclusion complex formation between HPG-PCL-MPEG and α-CD, which resulted in a supramolecular-structured hydrogel [30]. The α-CD first interacted with PEG segments to form the necklace-like inclusion complexes, and one PEG segments could interact with several α-CD molecules [31,32]. Then the formed inclusion complexes interacted to each other by hydrogen bond coming from the abundant hydroxyl groups of α-CD, which form the crosslink points of the hydrogels. To confirm this, X-ray diffraction (XRD) measurement was conducted for α-CD, HPG-PCL-MPEG and the resultant supramolecular hydrogel. From the XRD patterns shown in Fig. 5, the hydrogel sample was observed to have two characteristic diffraction peaks at 2θ = 19.8° (d = 4.44 Å) and 22.6° (d = 3.94 Å), which were not observed in the patterns of HPG-PCL-MPEG and α-CD, and were assigned to the {210} and {300} reflections from the hexagonal lattice with a = 13.6 Å. The strong {210} reflection is a typical peak observed for the polymer inclusion complexes with α-CD [33]. These results demonstrate the existence of the HPG-PCL-MPEG/α-CD inclusion complexes, in which α-CD threaded onto the MPEG segments to form the physical crosslinks and induce the formation of the supramolecular hydrogel networks.

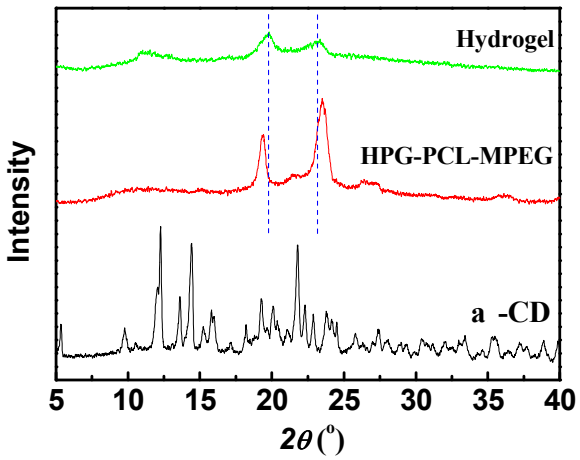

Fig. 5. XRD patterns of α-CD, HPG-PCL-MPEG and the supramolecular hydrogel.

Moreover, the gelation time was dependent on α-CD concentration. To modulate the rate and extent of the gelation in such a supramolecular system, we investigated the effect of α-CD concentration on the gelation kinetics by rheological monitoring. To ensure the dynamic measurement within linear viscoelastic region, dynamic strain test was carried out firstly, and then the strain was set to be 0.1%. Then, a time sweep measurement for the viscoelastic property was carried out, in which the storage modulus (G') and loss modulus (G'') were monitored as a function of time. Fig. 6 showed the time dependence of G' and G'' for three samples with different α-CD concentrations. When 2.0% α-CD was used, it was found that the values of G' and G'' were neglectable and overlapped at the early time. In particular, a crossover point between G' and G'' was observed at the time of 56.3 minutes, which implied that there was a sol–gel transition (Fig. 6A). Beyond the crossing, the G' value became larger than the G'' value, indicating that the system became more elastic. The corresponding time of the crossover from a viscous behavior to an elastic response could be regarded as the gelation time [34]. The gelation time was recorded to be 16.8 minutes in the case of 4.0% α-CD in mixture system. And in the case of 6.0% α-CD, the gelation transition occurred in 2 minutes. In this case, the G' value was observed to be larger than the G'' value in the time range investigated, showing a dominant elastic property. It is clear that the gelation time of this supramolecular system decreased with the increase of α-CD concentration.

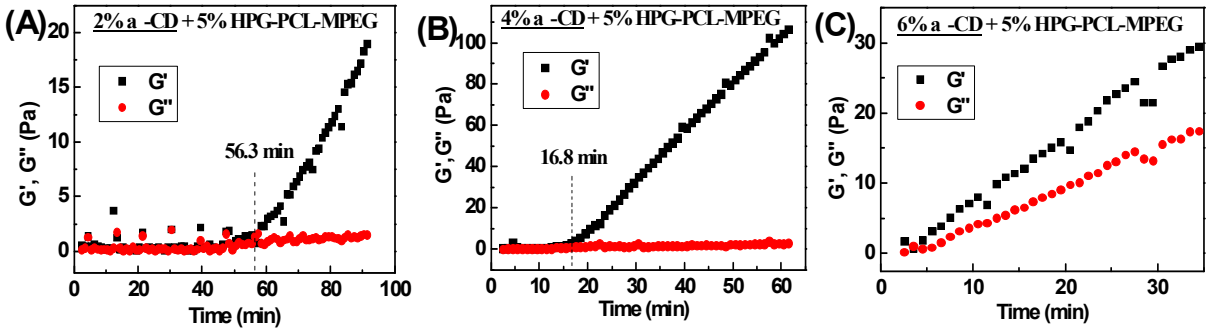

Fig. 6. Effect of the α-CD concentration on the gelation time (1.0 rad/s frequency, 0.1% strain and 25 °C).

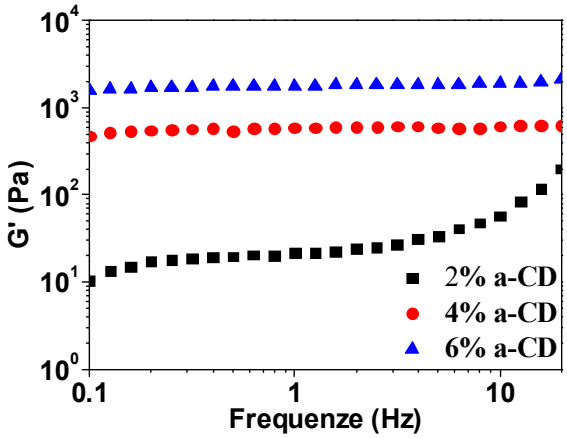

Fig. 7. Effects of α-CD concentration on the hydrogel strength (0.1% strain, 25 ºC).

Further studies were carried out to understand the effect of α-CD concentration on the hydrogel strength for the gelled HPG-PCL-MPEG/α-CD systems, as shown in Fig. 7. It was found that an increase of α-CD concentration could result in an enhancement of the elastic modulus. This may be attributed to the fact that a higher concentration of α-CD would be favorable for the formation of the supromolecular hydrogel with high mechanical strength due to the enhanced inclusion complexation [35].

3.2. *In vitro* synergistic effect of DOX and CPT

To confirm the synergistic effect of co-loaded DOX and CPT, we evaluated the *in vitro* cytotoxicity of the dual-drug loaded micelles using MTT assay. Firstly, the blank micelles were tested and no cytotoxicity to HNE-1 cells was found after 48 h incubation. Therefore, the micelles

were well tolerated and safe to HNE-1 cells under the experimental concentration. The inhibition ratios of used drug-loaded micelles were shown in Table 1, and the following results were obtained: (1) all the drug-loaded micelles showed dose-dependent cell proliferation inhibition behavior; (2) the drug combination effect was observed.

Table 1. Inhibition ratios of CPT, DOX, and CPT combined DOX to HNE-1 cells at 48 h.

Corresponding DOX/CPT concentration (μg/mL)	Inhibition ratio (%)		
	DOX (%)	CPT (%)	DOX+CPT (%)
0.02/0.03	3.95±0.41	2.72±0.29	7.92±0.68*
0.05/0.075	6.75±1.22	6.77±0.89	15.26±1.71*
0.1/0.15	14.95±3.40	12.11±1.11	24.25±5.49*
0.2/0.3	17.38±3.27	17.68±2.26	34.28±3.82*
0.5/0.75	25.93±0.93	27.73±4.32	47.97±3.95*
1/1.5	32.06±2.78	35.54±2.14	62.44±4.61*
2/3	45.01±0.69	48.62±2.53	70.11±1.73*
5/7.5	58.45±1.82	60.54±2.06	73.49±2.28*

*P <0.05. HPG-PCL-MPEG with concentration range of 0.05-0.50 mg/mL has no significant difference with PBS control in cell viability.

The CI plots dose-normalized isobologram analyses shown in Fig. 8 helped us to evaluate the drug combination effect. In CI plots, combination index, derived from the dose-effect profiles of a given drug combination Table 1, was plotted against drug effect level. Such a plot can provide quantitative information about the extent of drug interactions, with CI values lower than, equal to or higher than 1 denoting synergism, additivity or antagonism, respectively [36]. As shown in Fig. 8, CI values showed lower than 1 at the experimental concentration range, demonstrating high synergism effect against HNE-1 cells. Moreover, CI values decreased with the increase of inhibition ratios, demonstrated that the DOX and CPT-loaded micelles showed better synergism efficiency at higher drug effect levels. These results provide good foundations for further evaluation.

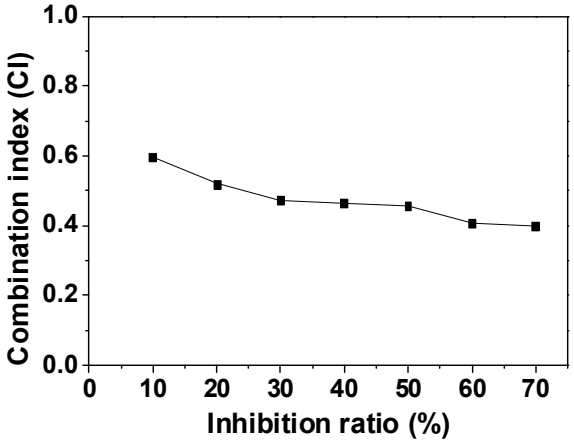

Fig. 8. Plot of the combination index (CI) as the function of cell inhibition ratio for HNE-1 cells treated with DOX and CPT combination.

3.3. Drug release, *in vitro* and *in vivo* synergistic assays

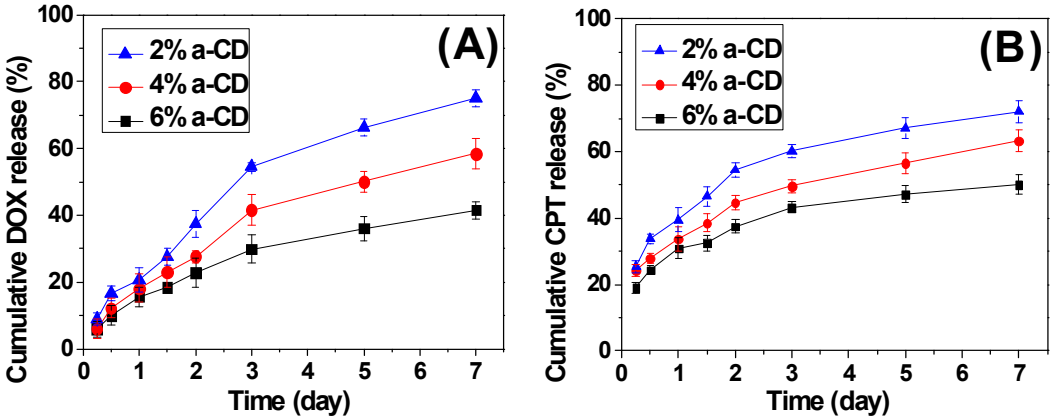

Fig. 9. *In vitro* DOX and CPT release profiles from supramolecular hydrogels with different α-CD concentrations.

The application of this supramolecular hydrogel as a new injectable drug delivery system for the controlled and sustained release of CPT and DOX was investigated. Fig. 9 showed the *in vitro* release profiles for loaded CPT and DOX released from HPG-PCL-MPEG/CPT/DOX/α-CD supramolecular hydrogels with different α-CD concentration in PBS at 37 ºC. In all cases, CPT and DOX could be released simultaneously and no initial burst release was observed. Depending on α-CD concentration used for the hydrogel formation, various release rates were found for loaded

CPT and DOX respectively. The CPT or DOX release rate decreased with the increase of α-CD concentration. This phenomenon could be explained by considering the greater gelation extent and the formation of denser hydrogel network in the case of the higher a-CD amount, which hindered the release of loaded drugs from the supramolecular hydrogel.

To understand the release mechanism of loaded CPT and DOX, we fitted the accumulative release data using the following semiempirical equation [37]:

$M_t / M_\infty = K t^n$ (for $M_t/M_\infty \leq 0.6$)

where M_t and M_∞ are the cumulative amount of the drug released at t and equilibium, respectively; k is the rate constant relating to the properties of the hydrogel matrix and the drug, and n is the release exponent characterizing the transport mechanism. According to this classification, there are four distinguishable modes of diffusion: (i) the value of n = 0.5 suggests Fickian or Case I transport behaviour in which the relaxation coefficient is negligible during transient sorption; (ii) the value of n=1 refers to a non-Fickian or Case II mode of transport where the morphological changes are abrupt; (iii) if $0.5 < n < 1$, the transport process is anomalous, corresponding to Case III, and the structural relaxation is comparable to diffusion; (iv) a value of $n < 0.5$ indicates a pseudo-Fickian behavior of diffusion where sorption curves resemble Fickian curves, but the approach to final equilibrium is very slow.

Table 2 Release characteristics of encapsulated DOX and CPT from HPG-PCL-PEG/α-CD supramolecular hydrogels with different α-CD concentration.

Hydrogel composition	*k*	*n*	R^2	Transport mechanism
DOX release:				
2% α-CD	1.42	0.35	0.995	pseudo-Fickian
4% α-CD	1.31	0.32	0.996	pseudo-Fickian
6% α-CD	1.23	0.30	0.989	pseudo-Fickian
CPT release:				
2% α-CD	1.40	0.28	0.989	pseudo-Fickian
4% α-CD	1.26	0.25	0.992	pseudo-Fickian
6% α-CD	1.22	0.22	0.995	pseudo-Fickian

By plotting $\log(M_t/M_\infty)$ versus $\log(t)$, the n and k values as well as the corresponding determination coefficients (R^2) were obtained, as listed in Table 2. The k values were found to

decrease with the increase of α-CD concentration. This phenomenon could be explained by considering the greater gelation extent and the formation of denser hydrogel network in the case of higher α-CD concentration, which hindered the dual-drug release and avoided supramolecular hydrogel erosion. In addition, the *n* values in all hydrogel cases were found to be in the range from 0.22 to 0.35, showing a pseudo-Fickian mechanism.

To confirm whether the released CPT and DOX could induce cell death effectively, the percentage of cell apoptosis treated with various formulations was determined by flow cytometer. Annexin V-FITC staining in conjunction with PI can distinguish early apoptosis from late apoptosis or living cells from necrotic cells [38]. As shown in Fig. 10, after incubation with HPG-PCL-MPEG for 48 h, HNE-1 cells displayed limited cell death compared with control group, which was consistent with the observed results of cytotoxicity analysis, demonstrating the good biocompatibility of HPG-PCL-MPEG. Cells treated with released CPT or DOX from supramolecular hydrogels exhibited the obvious increase of necrosis. The percentage of necrosis of HPG-PCL-MPEG/CPT treated cells was 29.6%. Similarly, HPG-PCL-MPEG/DOX caused 15.4% of cell necrosis. For the released HPG-PCL-MPEG/CPT/DOX, the necrosis percentage reached up to 53.4%, which was much more than the sum of individual CPT and DOX used. Recently, new clinical therapeutic strategy to tumor has been mainly focused on inducing the tumor cells apoptosis, because it is reported that this strategy can not cause inflammatory reaction [39]. However, this strategy may induce immune suppression, and also the tumor recurrence due to the horizontal transmission of gene from devoured apoptosis cells. So, some reports proposed that the tumor treatment strategy should be turn in to promoting tumor cell necrosis and inducing anti-tumor immune responses [40,41]. The result from this work revealed that CPT combined with DOX significantly enhanced the cell death, in other words, the codelivering strategy is a promising method in cancer therapy.

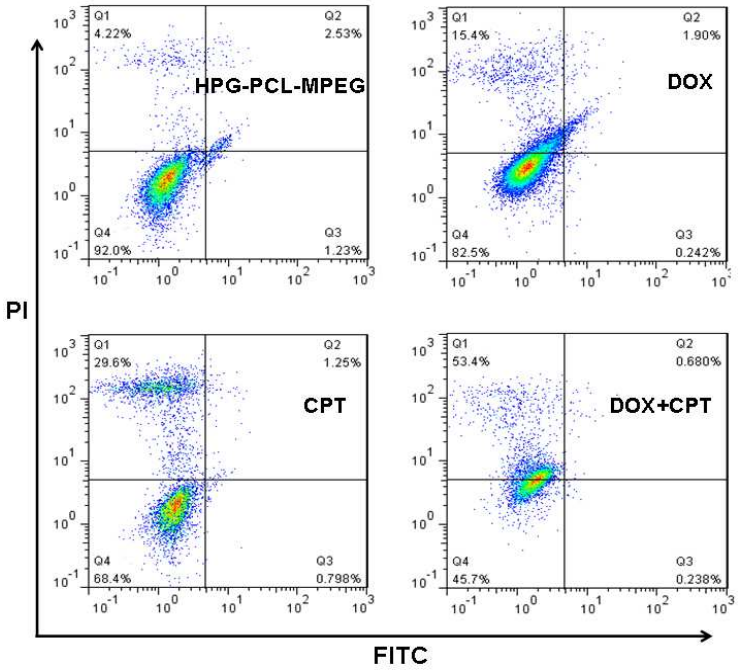

Fig. 10. Apoptosis analysis by flow cytometry after HNE-1 cells incubated with blank HPG-PCL-MPEG, released CPT, released DOX and released CPT/DOX.

Fig. 11. Photograph of the tumor at the 21th day after treatment of various formulations.

The anti-tumor effect *in vivo* of CPT, DOX or CPT/DOX loaded hydrogels was tested, and PBS and blank hydrogel were used as the control. The representative tumor images were shown in Fig. 11. As seen, the tumor volume of PBS treatment group increased rapidly, and had no significant difference in volume with blank hydrogel sample. However, all the chemotherapy groups were effective in tumor regression. In detail, dur to the synergistic effect, the combined CPT and DOX exhibited better tumor inhibition than individual CPT or DOX, indicating the superiority of combined chemotherapy.

3.4. Biocompatibility

The nonspecific interactions of biomaterials with blood components could severely diminish the half-life and targetability of complexes [42]. The blood compatibility of the supramolecular hydrogel was assessed by spectrophotometric measurement of hemoglobin release from erythrocytes after polymer treatment. Fig. 12 showed the percentage hemolysis of blood in contact with α-CD, HPG-PCL-MPEG and resultant supramolecular hydrogel with different incubation time. It was found that α-CD caused serious hemolysis rapidly as a result of the erythrocyte membrane disruption, while HPG-PCL-MPEG showed a much better blood compatibility with the extent of hemolysis lower than the permissible level of 5% for 12 h. After the interaction between α-CD and HPG-PCL-MPEG, the supramolecular hydrogel showed the good blood compatibility at the initial 9 h. However, the 8% hemolysis at 12 h for supramolecular hydrogel was higher, which may be resulted from the sustained α-CD release induced by hydrogel degradation. Compared with some reported blood-compatible hydrogels which are usually covered by blood-compatible [43], our hydrogels showed the receivable blood compatibility. Moreover, if the supramolecular hydrogel was used *in vivo*, the degradation product could be cleared sustainedly by the interstitial fluid or blood, which could confirm the blood safety of the supramolecular hydrogel.

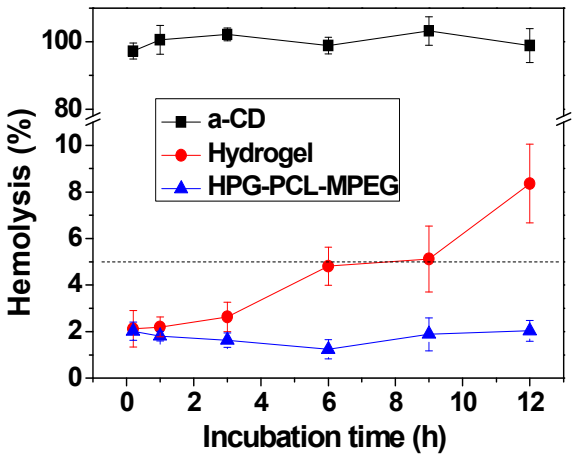

Fig. 12 The hemolysis of HPG-PCL-MPEG, α-CD and the resultant hydrogel.

The cytotoxicity of the supramolecular hydrogel was evaluated on HNE-1 cells by an MTT assay. Fig. 13 gave the cell viability result of the HNE-1 cells cultured in the media treated with the extracts of supramolecular hydrogels with various concentrations. As seen, the treated HNE-1 cells

showed high cell viability comparable to that of the control cells, regardless of cultured time. As most reported publishers [44], no significant difference ($p < 0.05$) in the cell viability was observed among the cells treated with PBS and the hydrogel extracts. These results indicate that the used supramolecular hydrogel matrices are non-cytotoxic and have a good biocompatibility.

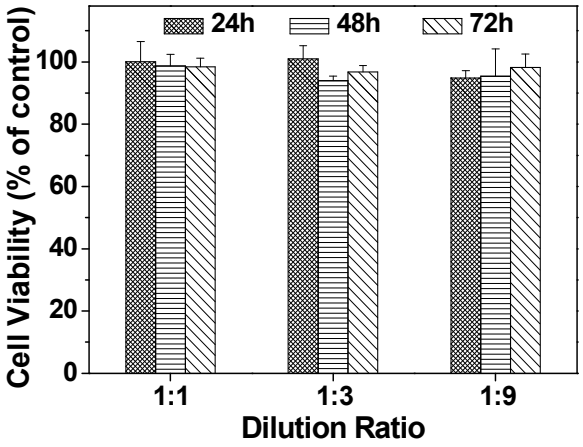

Fig. 13 MTT results of hydrogels on HNE-1 cells.

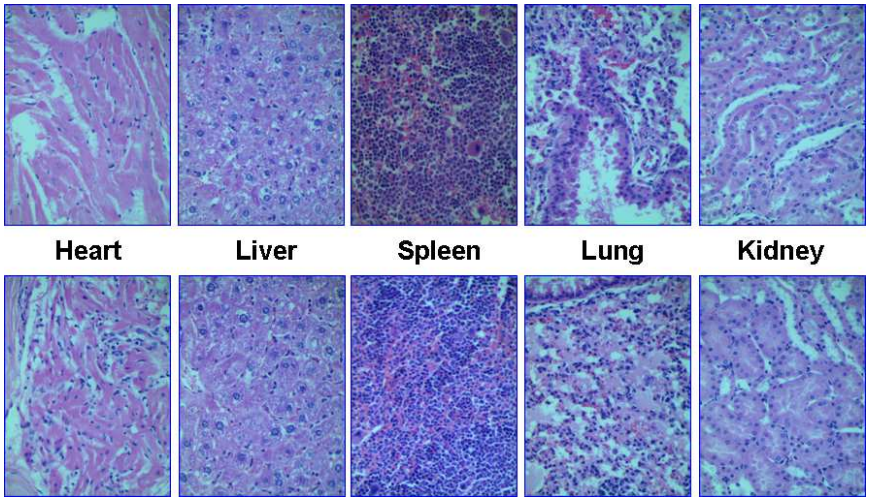

Fig. 14. Representative organ histology for PBS control (top row) and supramolecular hydrogel (bottom row) from injected rats.

In vivo toxicity studies are essential to prove the safety of the supramolecular hydrogel used as drug carriers. Herin, a histological analysis of organs was performed to determine whether the supramolecular hydrogel caused tissue damage, inflammation, or lesions. As shown in Fig. 14,

histologically, no visible difference was observed compared to the control (top row). The *in vivo* toxicity of materials is influenced by the chemical structures, size, exposure duration, biodistribution, location, metabolism as well as the nature of the surface and terminal groups [45]. The non-observed toxicity of the supramolecular hydrogel could be attributed to its degradation and lower molecular weight (less than 10 KDa) of degraded products. Usually, the supramolecular hydrogel could first degrade as HPG-PCL-MPEG and α-CD, and then HPG-PCL-MPEG and α-CD could degrade further as smaller molecules, and also the degraded products showed good biocompatibility. So, this supramolecular showed excellent biocompatibility.

4. Conclusion

A supramolecular hydrogel which could co-load and sustainedly release CPT and DOX was prepared by the host-guest interactions between α-CD and HPG-PCL-MPEG. Their gelation kinetics and hydrogel strength have been studied by dynamic and steady rheometry under various concentration of *α*-CD, which indicated that their physical properties could be modulated by *α*-CD concentration. And the sustained dual drug release from supramolecular hydrogel was also adjusted by *α*-CD concentration. For further investigation, the loaded CPT and DOX showed the synergistic effect obviously *in vitro* and *in vivo*, which could induce HNE-1 cells death and inhibit tumor effectively. Moreover, the supramolecular hydrogel showed a receivable blood compatibility and non-cytotoxity by *in vitro* and *in vivo* assays. Therefore, this supramolecular hydrogel have a potential application in sustainedly synergistic tumor therapy.

Acknowledgements

This work was financially supported by National Natural Science Foundation of China (31271019, 21104099 and 81260406) as well as Natural Science Foundation of Guangdong Province (S2013010013452).

References

[1] M. Saraswathy and S. Q. Gong, Mater. Today, 2014, 17, 298.

[2] D. Ma, Q. M. Lin, L. M. Zhang, Y. Y. Liang and W. Xue, Biomaterials, 2014, 35, 4357.

[3] H. Y. Wang, Q. Q. Guo, Y. F. Jiang, E. G. Liu, Y. X. Zhao, H. X. Wang, Y. P. Li and Y. Z.

Huang, Adv. Funct. Mater., 2013, 23, 6068.

[4] D. Ma, K. Tu and L. M. Zhang, Biomacromolecules, 2010, 11, 2204.

[5] S. Aryal, C. M. J. Hu and L. F. Zhang, Small, 2010, 13, 1442.

[6] T. Liu, W. Xue, B. Ke, M. Q. Xie and D. Ma, Biomaterials, 2014, 35, 3865.

[7] S. H. Allan, Adv. Drug Deliver. Rev., 2002, 43, 3.

[8] N. K. Christian, A. N. Wilson, C. B. Dong, C. Z. Dinu, G. A. Justin and G. E. Anthony, Biomaterials, 2013, 34, 6318.

[9] G. E.. Anthony, C. B. Dong and C. Z. Dinu, J. Mater. Chem., 2012, 22, 19529.

[10] S. H. Seo, H. D. Han, K. H. Noh, T. W. Kim and S. W. Son, Clin. Exp. Metastas., 2009, 26, 179.

[11] S. P. Patil, H. S. Jeong and H. Kim, Chem. Commu., 2012, 48, 8901.

[12] L. Mao, H. Wang, M. Tan, L. Ou, D. Kong and Z. Yang, Chem. Commu., 2012, 48, 395.

[13] H. Akira, T. Yoshinori and N. Masaki, Acc. Chem. Res., 2014, 47, 2128.

[14] H. T. Cui, L. G. Cui, P. B. Zhang, Y. B. Huang and X. S. Chen, Macromol. Biosci., 2014, 14, 440.

[15] H. H. Kuang, H. Y. He, Z. Y. Zhang, Y. X. Qi, Z. G. Xie, X. B. Jing and Y. B. Huang, J. Mater. Chem. B, 2014, 2, 659.

[16] D. Ma, T.Wu, J. L. Zhang, M. S. Lin, W. J. Mai, S. Z. Tan, W. Xue and X. Cai, Sci. Adv. Mater., 2013, 5, 1400.

[17] L. P. Zhou, J. X. Li, Q. Luo, J. Y. Zhu, H. X. Zou, Y. Z. Gao, L. Wang, J. Y. Xu, Z. Y. Dong and J. Q. Liu, Soft Matter, 2013, 9, 4635.

[18] Z. C. Tian, C. Chen and R. A. Harry, Macromolecules, 2013, 46, 2715.

[19] D. Ma, H. B. Zhang, K. Tu and L. M. Zhang, Soft Matter, 2012, 8, 3665.

[20] X. J. Zhang, X. G. Zhang, Z. G. Wu, X. J. Gao, C. Cheng, Z. Wang and C. X. Li, Acta Biomater., 2011, 7, 585.

[21] A. S. Rajesh, F. L. Benjamin, I. U. Muhammad, E. B. Donald and N. K. Jayachandran, Biomaterials, 2013, 34, 6068.

[22] D. Ma, L. M. Zhang, X. Xie, T. Liu and M. Q. Xie, J. Colloid Interf. Sci., 2011, 359, 399.

[23] K. K. Rajesh, J. Johan, N. K. Jayachandran, V. D. Dana and E. B. Donald, Biomaterials, 2008, 29, 1693.

[24] X. L. Yang, Y. L. Luo, F. Xu and Y. S. Chen, Pharm. Res., 2014, 31, 291.

[25] Y. P. Chen, Y. Y. Qi and B. Liu, J. Nanomater., 2013, Article ID 345738.

[26] R. S. Benjamin, M. I. Ghare, C.Bhattacharya, R. Paul, Z.Q. Yu, P. A. Zaleski, T. C. Bozeman, M. J. Rishel, and S. M. Hecht,J. Am. Chem. Soc., 2014, 136, 13641.

[27] W. T. Song, Z. H.Tang, M. Q. Li, S. X. Lv, H. Sun, M. X. Deng, H. Y. Liu and X. S. Chen, Acta Biomater., 2014, 10,1392.

[28] R. P.O'Leary and W. L. Guess, J. pharm. Sci., 1968, 57, 12.

[29] N. K. Indah, H. Liang, K. Sumit, M. Andreas, K. S. Sunil, P. R. Jürgen and H. Rainer,J. Mater. Chem. B, 2013, 1, 3569.

[30] A. Harada, J. Li and M. Kamachi, J. Am. Chem. Soc., 1994, 8, 3192.

[31] M. V. Rekharsky and Y. Inoue, Chem. Rev. , 1998, 98, 1875.

[32] J. Lu, P. A. Mirau and A. E. Tonelli, Prog. Polym. Sci., 2002, 27, 357.

[33] K. M. Huh, T.Ooya, S. Sasaki and N. Yui, Macromolecules, 2001, 34, 2402.

[34] H. H. Winter and F. Chambon, J. Rheol., 1986, 30, 367.

[35] A. Harada, J. Li and M. Kamachi, Macromolecules, 1993, 26, 5698.

[36] H. H. P. Duong and L. Y. Yung, Int. J. Pharm., 2013, 454, 486.

[37] N. W. Franson and N. A. Peppas, J. Appl. Polym. Sci. 1983, 28, 1299.

[38] H. J. Byeon, S. H. Choi, J. S. Choi, I. Kim, B. S. Shin and E. S. Lee, Acta Biomater., 2014, 10, 142.

[39] Y. Q. Guan, Z. Zheng, Z. B. Li and J. M. Liu,Acta Biomater., 2012, 8, 1348.

[40] B.Fadeel,Cell. Mol. Life Sci., 2003, 60, 2575.

[41] P. Davidovich, C. J. Kearney and S. J. Martin, Biol. Chem., 2014, 395, 1163.

[42] J. Yang, Y. Liu, H. Wang, L. Liu, W. Wang and C. Wang, Biomaterials, 2012, 33, 604.

[43] Y. Xia, C. Cheng, R. Wang, H. Qin, Y. Zhang, L. Ma, H. Tan, Z. W. Gu and C. S. Zhao, Polym. Chem., 2014, 5, 5906.

[44] F. Yang, J. Wang, L. Y. Cao, R. Chen, L. J. Tang and C. S. Liu, J. Mater. Chem. B, 2014, 2, 295.

[45] K. Luo, C. X. Li, L. Li, W. C. She, G. Wang and Z. W. Gu, Biomaterials, 2012, 33, 4917.

Colour graphic

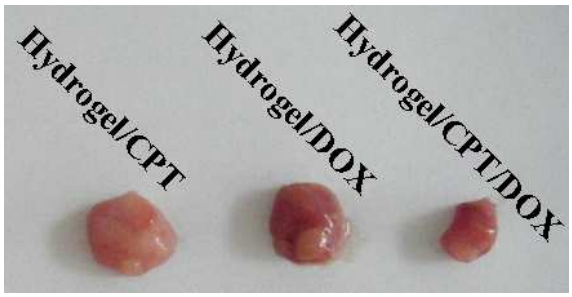

Text

A supramolecular hydrogel was prepared to encapsulate and controlled release both camptothecine and doxorubicin for sustainedly synergistic tumor therapy.